

## Durham Research Online

---

### Deposited in DRO:

19 October 2015

### Version of attached file:

Accepted Version

### Peer-review status of attached file:

Peer-reviewed

### Citation for published item:

Chandler, B.M.P. and Evans, D.J.A. and Roberts, D.H. and Ewertowski, M. and Clayton, A.I. (2016) 'Glacial geomorphology of the Skálafellsjökull foreland, Iceland : a case study of 'annual' moraines.', *Journal of maps.*, 12 (5). pp. 904-916.

### Further information on publisher's website:

<http://dx.doi.org/10.1080/17445647.2015.1096216>

### Publisher's copyright statement:

This is an Accepted Manuscript of an article published by Taylor Francis Group in *Journal of Maps* on 11/10/2015, available online at: <http://www.tandfonline.com/10.1080/17445647.2015.1096216>.

### Additional information:

---

### Use policy

The full-text may be used and/or reproduced, and given to third parties in any format or medium, without prior permission or charge, for personal research or study, educational, or not-for-profit purposes provided that:

- a full bibliographic reference is made to the original source
- a [link](#) is made to the metadata record in DRO
- the full-text is not changed in any way

The full-text must not be sold in any format or medium without the formal permission of the copyright holders.

Please consult the [full DRO policy](#) for further details.



**Glacial geomorphology of the Skálafellsjökull foreland,  
Iceland: a case study of "annual" moraines**

Journal:	<i>Journal of Maps</i>
Manuscript ID:	TJOM-2015-0090
Manuscript Type:	Original Article
Date Submitted by the Author:	02-Jun-2015
Complete List of Authors:	Chandler, Benjamin; Queen Mary University of London, School of Geography Evans, David, John, Alexander; University of Durham, Geography Roberts, David; University of Durham, Geography Ewertowski, Marek; University of Durham, Geography Clayton, Alexander; University of Southampton, Geography and Environment
Keywords:	glacial geomorphology, remote sensing, "annual" moraines, active temperate glacial landsystem, Skálafellsjökull, Iceland

SCHOLARONE™  
Manuscripts

1  
2  
3  
4  
5  
6  
7  
8  
9  
10  
11  
12  
13  
14  
15  
16  
17  
18  
19  
20  
21  
22  
23  
24  
25  
26  
27  
28  
29  
30  
31  
32  
33  
34  
35  
36  
37  
38  
39  
40  
41  
42  
43  
44  
45  
46  
47  
48  
49  
50  
51  
52  
53  
54  
55  
56  
57  
58  
59  
60

**1      Glacial geomorphology of the Skálafellsjökull foreland, Iceland: a**  
**2      case study of “annual” moraines**

3  
4      Benjamin M.P. Chandler<sup>1</sup> \*, David J.A. Evans<sup>1</sup>, David H. Roberts<sup>1</sup>, Marek W. Ewertowski<sup>1</sup>  
5      and Alexander I. Clayton<sup>2</sup>

6  
7      <sup>1</sup> Department of Geography, Durham University, Durham, UK

8  
9      <sup>2</sup> Geography and Environment, University of Southampton, Southampton, UK

10  
11      \* Correspondence to: Benjamin M.P. Chandler, School of Geography, Queen Mary  
12      University of London, Mile End Road, London, E1 4NS, UK. Email:  
13      [b.m.p.chandler@qmul.ac.uk](mailto:b.m.p.chandler@qmul.ac.uk)

# Glacial geomorphology of the Skálafellsjökull foreland, Iceland: a case study of “annual” moraines

## Abstract

Small-scale recessional (“annual”) moraines are a characteristic signature of the active temperate glacial landsystem. These “annual” moraines represent a potentially valuable terrestrial climate archive, and may provide valuable insights into glacier dynamics. This paper presents detailed glacial geomorphological maps of “annual” moraines on the foreland of Skálafellsjökull, SE Iceland. Geomorphological maps have been produced at a scale of 1:3,750 based on 2006 aerial photographs and 2012 satellite imagery. Using UAV-captured imagery, large-scale sample maps of two selected areas of the glacier foreland have also been produced at scales of 1:850 and 1:750, respectively. Desk- and field-based mapping reveals suites of recessional (“annual”) moraines distributed across the glacier foreland, often found in close association with flutings. Moraines on the foreland typically display distinctive “sawtooth” planform geometries, with complexities in the pattern occurring due to localised superimposition. The inventory of glacial geomorphological maps presented here provides a framework for subsequently exploring the characteristics of the “annual” moraines and recent ice-marginal fluctuations at Skálafellsjökull.

**Keywords:** glacial geomorphology; remote sensing; “annual” moraines; active temperate glacial landsystem; Skálafellsjökull; Iceland



1  
2  
3  
4  
5  
6  
7  
8  
9  
10  
11  
12  
13  
14  
15  
16  
17  
18  
19  
20  
21  
22  
23  
24  
25  
26  
27  
28  
29  
30  
31  
32  
33  
34  
35  
36  
37  
38  
39  
40  
41  
42  
43  
44  
45  
46  
47  
48  
49  
50  
51  
52  
53  
54  
55  
56  
57  
58  
59  
60

**1. Introduction**

Annual ice-marginal fluctuations at many Icelandic glaciers are manifest in the form of annual (push/squeeze) moraines (e.g. Price, 1970; Sharp, 1984; Krüger, 1995; Evans and Twigg, 2002), a characteristic signature of the active temperate glacial landsystem (Evans, 2003, 2005; Evans and Orton, 2015). Annual moraine formation occurs at the ice-margin during a period when forward ice-front movement exceeds the negligible ablation during the winter (Lukas, 2012; Bradwell et al., 2013). Long sequences of annual moraines form when ice-front recession during the summer (ablation season) outstrips advance during the winter (accumulation season) over the course of a number of years (Boulton 1986; Bennett 2001). Long sequences of annual moraines potentially contain a seasonal signature of glacier response to climatic fluctuations, and have been associated with periods of elevated ablation-season temperature (Sharp, 1984; Krüger, 1995; Bradwell, 2004; Beedle et al., 2009; Bradwell et al., 2013). Given the potential of these features as a terrestrial climate archive, detailed examination of the characteristics of annual moraines on the forelands of Icelandic glaciers could yield valuable insights into the nature of, and controls on, recent ice-marginal retreat. During the past decade Icelandic glaciers have exhibited accelerating rates of ice-marginal retreat and mass loss (e.g. Sigurðsson et al., 2007; Björnsson et al., 2013). Understanding this current rapid glacier change is crucial to placing current atmospheric warming and associated glacier retreat in a broader context. This study presents detailed mapping of “annual” moraines on the foreland of Skálafellsjökull, SE Iceland, with the intention of providing a framework to examine: (i) the moraine characteristics (geomorphology, genesis and chronology) in detail; and (ii) patterns and rates of ice-marginal retreat at this outlet glacier. These “annual” moraines have previously been argued to form on an annual basis through seasonally-driven ice-marginal processes (cf. Sharp, 1984), and the detailed mapping will therefore also provide a basis for re-examining this concept.

75

## 76 2. Study site and previous work

### 77 2.1 Study site

78 Skálafellsjökull, a non-surging outlet of the southeastern margin of the Vatnajökull ice-cap in  
79 SE Iceland, flows for ~25 km from the Breiðabunga plateau in eastern Vatnajökull (Figure 1).  
80 The glacier descends steeply from the lava plateau onto a low elevation foreland, where it  
81 splays out to form a piedmont lobe. The current ice-margin terminates at an altitude of ~60 m  
82 a.s.l. on the Hornafjörður coastal plain (McKinze et al., 2004; Evans and Orton, 2015). At  
83 its northern margin, the glacier is topographically confined by the Hafrællsháls mountain  
84 spur, which reaches a maximum elevation of ~1008 m a.s.l. (Evans and Orton, 2015). The  
85 contemporary Skálafellsjökull ice-margin is fronted by two proglacial lakes, the largest  
86 situated on Heinabergsvötn (Figure 1c), and a smaller proglacial lake at the southeastern  
87 sector of the ice-margin.

88

89 Documentary evidence and maps indicate that Skálafellsjökull formerly coalesced with the  
90 neighbouring Heinabergsjökull, and they remained confluent until sometime between 1929  
91 and 1945 (cf. Thórarinnsson, 1943; Hannesdóttir et al., 2014, and references therein). Ice-front  
92 measurements conducted at the glacier since the 1930s indicate Skálafellsjökull underwent  
93 similar fluctuations to other non-surge-type Vatnajökull outlet glaciers (e.g. Sigurðsson,  
94 1998). Since the 1970s, however, measurements have been sporadic, limiting understanding  
95 of glacier change at Skálafellsjökull during this period. Thus, the sequences of recessional  
96 (“annual”) moraines previously identified on the Skálafellsjökull foreland (Sharp, 1984;  
97 Evans and Orton, 2015) offer the opportunity to gain important insights into ice-frontal  
98 fluctuations.

99

1  
2  
3  
4  
5  
6  
7  
8  
9  
10  
11  
12  
13  
14  
15  
16  
17  
18  
19  
20  
21  
22  
23  
24  
25  
26  
27  
28  
29  
30  
31  
32  
33  
34  
35  
36  
37  
38  
39  
40  
41  
42  
43  
44  
45  
46  
47  
48  
49  
50  
51  
52  
53  
54  
55  
56  
57  
58  
59  
60

100    **2.2 Previous mapping**

101    Skálafellsjökull has been the subject of a number of studies, including the investigation of the  
102    glacial landsystem as whole (Evans and Orton, 2015), component sediment-landform  
103    assemblages (Sharp, 1984; Dowdeswell and Sharp, 1986; Evans, 2000) and the timing of LIA  
104    maxima (e.g. Gordon and Sharp, 1983; Evans et al., 1999; McKinzey et al., 2004). In a recent  
105    study, Evans and Orton (2015) mapped the surficial geology and glacial geomorphology of  
106    the Skálafellsjökull foreland, and neighbouring Heinabergsjökull foreland. Evans and Orton  
107    (2015) established that the Skálafellsjökull glacier foreland constitutes a landsystem imprint  
108    of actively retreating temperate glaciers in a mountain environment with a high glaciofluvial  
109    sediment yield. Moreover, the landsystem is characterised by the three diagnostic  
110    depositional domains of the active temperate landsystem previously identified for Icelandic  
111    piedmont lobes: marginal morainic, subglacial and glaciofluvial/glaciolacustrine (Krüger,  
112    1994; Evans and Twigg, 2002; Evans, 2003, and references therein). The Skálafellsjökull  
113    glacier foreland also contains site-specific sediment-landform assemblages, notably  
114    overridden kame terraces on the southern part of the foreland. The survival of kame terraces  
115    is unusual and therefore the fluted kame terraces at Skálafellsjökull provide an important  
116    modern analogue for studies on palimpsest glacial landscapes, which are traditionally  
117    assumed to be produced by cold-based conditions in contrast to the wet-based conditions at  
118    Skálafellsjökull (e.g. Forman et al., 1987; Hättestrand and Stroeven, 2002; Landvik et al.,  
119    2005; Davis et al., 2006). The combined landform record of Skálafellsjökull and  
120    Heinabergsjökull constitutes a modern glacial landsystem analogue for active temperate  
121    piedmont lobes associated with the construction of large outwash heads fed by high  
122    glaciofluvial sediment yields (Evans and Orton, 2015).

123

1  
2  
3 124 Research focused on the marginal morainic domain of the Skálafellsjökull foreland has  
4  
5  
6 125 previously been conducted by Sharp (1984). The study specifically examined a sequence of  
7  
8 126 “annual” moraines within the southern part of the foreland, located in an area of roches  
9  
10 127 moutonnées and a discontinuous sheet of fluted subglacial traction till (*sensu* Evans et al.,  
11  
12 128 2006; Sharp, 1984; Evans and Orton, 2015). Sedimentological investigations by Sharp (1984)  
13  
14 129 identified four process combinations, argued to be forming moraine ridges on an annual basis  
15  
16 130 at the southeastern sector of the ice-margin. However, no detailed, large-scale mapping of the  
17  
18 131 intricate details of the “annual” moraines was presented.  
19  
20  
21  
22 132  
23  
24

### 25 133 **2.3 Purpose of the mapping**

26  
27  
28 134 The rationale for producing detailed maps of the “annual” moraines on the foreland of  
29  
30 135 Skálafellsjökull was twofold: (i) to provide context for examining the characteristics of these  
31  
32 136 features (moraine geomorphology, sedimentology and chronology) in detail; and (ii) to  
33  
34 137 provide a framework for investigating recent ice-marginal fluctuations using moraine  
35  
36 138 spacing. Importantly, the mapping, combined with additional sedimentological and  
37  
38 139 chronological analyses, will allow a re-examination of the concept of annual moraine  
39  
40 140 formation at Skálafellsjökull (cf. Sharp, 1984; Evans and Orton, 2015). The mapping also  
41  
42 141 aimed to build on the previous small-scale landsystem mapping undertaken by Evans and  
43  
44 142 Orton (2015). Individual maps have been produced at a scale of 1:3,750 based on the 2006  
45  
46 143 aerial photographs (Map 1) and 2012 satellite imagery (Map 2), providing a visual  
47  
48 144 demonstration of recent ice-marginal retreat and the evolution of the glacier foreland. In  
49  
50 145 addition to these two smaller-scale maps, detailed sample mapping of “annual” moraines has  
51  
52 146 been conducted based on hillshaded relief models generated from a 2013 high-resolution  
53  
54 147 DEM (Maps 3 and 4), allowing the complexity of “annual” moraine distribution and  
55  
56 148 geomorphology to be examined. These large-scale maps have been produced at scales of  
57  
58  
59  
60

1  
2  
3  
4  
5  
6  
7  
8  
9  
10  
11  
12  
13  
14  
15  
16  
17  
18  
19  
20  
21  
22  
23  
24  
25  
26  
27  
28  
29  
30  
31  
32  
33  
34  
35  
36  
37  
38  
39  
40  
41  
42  
43  
44  
45  
46  
47  
48  
49  
50  
51  
52  
53  
54  
55  
56  
57  
58  
59  
60

149 1:850 (Map 3) and 1:750 (Map 4), respectively. As the focus of the mapping was on the  
150 intricate details of the “annual” moraines, the maps do not include detailed mapping of the  
151 surficial geology. An indication of the distribution and coverage of glaciofluvial sediments is  
152 presented, though this mapped unit has been simplified so as not to detract from the detail of  
153 the mapped moraines. As highlighted above, mapping of the surficial geology has been  
154 presented by Evans and Orton (2015).

156 **3. Methods**

157 ***3.1 Remote sensing datasets and image preparation***

158 For the purposes of glacial geomorphological mapping, four remote sensing datasets were  
159 acquired (Figure 2). High-resolution scans of 2006 colour aerial photographs with a  
160 resolution of 0.41 m GSD (Ground Sample Distance) per pixel were obtained from the  
161 Icelandic survey company *Loftmyndir ehf*, whilst multispectral (8-band) and panchromatic  
162 satellite imagery captured by the WorldView-2 satellite sensor in June 2012 were acquired  
163 from *European Space Imaging*. The multispectral (8-band) satellite imagery and  
164 panchromatic images have resolutions of 2.0 m GSD and 0.5 m GSD, respectively. In  
165 addition, a further high-resolution remote sensing dataset has been used for mapping:  
166 specifically a Digital Elevation Model (DEM) with a spatial resolution of 0.09 m, derived  
167 from imagery captured using an Unmanned Aerial Vehicle (UAV) during aerial surveys of  
168 the Skálafellsjökull foreland in 2013 (see Hackney and Clayton, 2015). The images were  
169 taken using a fixed-wing QuestUAV 200 craft equipped with a mirrorless camera (Panasonic  
170 Lumix LX5 camera with 10.1 megapixel, 1/1.63 inch high-sensitivity CCD). Surveys were  
171 flown at an altitude of 100 m, yielding images with a resolution of 0.05 m GSD. A total of  
172 1,980 images were used to construct the DEM, selected on the basis of image quality and  
173 coherence of lighting. The final dataset of images used for processing had an approximate

1  
2  
3 174 photograph endlap of 80% and sidelap of 60%. However, the dataset does not provide  
4  
5 175 complete coverage of the Skálafellsjökull foreland, covering ~2 km<sup>2</sup> of the total area (~4.9  
6  
7  
8 176 km<sup>2</sup>) mapped. Thus, the 2006 aerial photographs and 2012 satellite imagery were largely  
9  
10 177 used in the composition of the smaller-scale geomorphological maps (Maps 1 and 2).  
11  
12  
13 178  
14  
15 179 Digital photogrammetric processing was conducted to remove the varying degrees of  
16  
17 180 geometric distortion inherent within aerial photographs (Lillesand et al., 2008; Campbell and  
18  
19 181 Wynne, 2011). For this purpose, both the 2006 aerial photographs and UAV-captured  
20  
21 182 imagery were processed in *Agisoft PhotoScan Professional Edition*, which utilises a  
22  
23 183 *Structure-from-Motion* (SfM) approach. SfM operates under the same basic principles as  
24  
25 184 stereoscopic photogrammetry, namely that 3D structure can be reconstructed from a series of  
26  
27 185 overlapping, offset two-dimensional images. However, it differs fundamentally from  
28  
29 186 conventional photogrammetry in that the geometry of the scene, camera positions and  
30  
31 187 orientation are solved automatically without the need to specify *a priori* a network of targets  
32  
33 188 with known 3D positions (Westoby et al., 2012). Instead, these are solved simultaneously  
34  
35 189 using an iterative bundle adjustment procedure, based on a database of features automatically  
36  
37 190 extracted from a set of multiple overlapping images (Snavely, 2008; Westoby et al., 2012;  
38  
39 191 Ryan et al., 2015). Position information can then be introduced after model production in an  
40  
41 192 arbitrary coordinate system, meaning that errors in ground control points (GCPs) will not  
42  
43 193 propagate in the DEM.  
44  
45  
46 194  
47  
48  
49  
50  
51  
52  
53 195 The first stage of processing in *Agisoft Photoscan* involves image alignment. The software  
54  
55 196 implements SfM algorithms to track features through a sequence of overlapping images in  
56  
57 197 order to estimate the relative location of camera positions for each image and generate a 3D  
58  
59 198 point-cloud of the tracked features (cf. Ryan et al., 2015, for further details). The point-cloud  
60

199 can subsequently be optimised and georeferenced using GCPs and/or using onboard  
 200 telemetry data. Following image alignment, a multi-view reconstruction algorithm is applied  
 201 to produce a 3D polygon mesh based on pixel values (Verhoeven, 2011; Ryan et al., 2015).  
 202 These 3D models can then be transformed and exported as DEMs and orthophotos. Using this  
 203 approach raster, grid DEMs with cell sizes of 0.41 m and 0.09 m were generated using the  
 204 2006 aerial photographs and 2013 UAV-imagery, respectively. An orthophoto mosaic of the  
 205 foreland, with a cell size of 0.41 m, was also produced using the 2006 model for the purposes  
 206 of landform mapping.  
 207  
 208 Positional ground control for the 2006 model was collected in the field using a Leica 1200  
 209 differential Global Positioning System (dGPS) between May and June 2014. The collected  
 210 ground control points (GCPs) were processed using the Canadian Spatial Reference System  
 211 Precise Point Positioning (CSRS-PPP: <http://webapp.geod.nrcan.gc.ca/geod/tools->  
 212 [outils/ppp.php?locale=en](http://webapp.geod.nrcan.gc.ca/geod/tools-)) tool, with the corrections then applied in *Leica Geo Office 8.3*. The  
 213 Coordinate Conversion and Datum Transformation in Iceland (cocodat<sup>i</sup>:  
 214 <http://cocodati.lmi.is/cocodati/cocodat-i.jsp>) tool was then employed to generate orthometric  
 215 heights for the GCPs and to convert the coordinates to UTM projected coordinates for zone  
 216 28N. Orthometric heights generated using the cocodat<sup>i</sup> tool are based on the ISN93 datum,  
 217 ellipsoid GRS80 and applies the new Icelandic geoid model. For practical purposes GRS80  
 218 and WGS1984 can be considered approximately equal, since there is a difference of only 0.1  
 219 mm in the semi-minor axis (cf. Rennen, 2004). The point-cloud generated in *Agisoft*  
 220 *PhotoScan* using the 2006 aerial photographs was optimised and georeferenced to WGS 1984  
 221 / UTM Zone 28N (ESPG: 32628) using the processed GCPs ( $n = 50$ ). This coordinate system  
 222 is compatible with the system currently employed by *Landmælingar Íslands* (National Land  
 223 Survey of Iceland) in the production of Icelandic maps. The UAV surveys were undertaken in



224 conjunction with a Leica dGPS deployed in Real-Time Kinematic (RTK) mode to allow  
225 georeferencing of the UAV-captured imagery (see Hackney and Clayton, 2015). Positional  
226 information for the UAV-imagery was provided by 15 GCPs located in a grid network across  
227 the surveyed area, with the model also georeferenced to WGS 1984 / UTM Zone 28N.  
228  
229 The satellite imagery obtained from *European Space Imaging* was purchased as *Ortho Ready*  
230 *Standard* and had been projected to UTM Zone 28N, spheroid WGS1984. The supplied  
231 imagery was orthorectified in *ArcMap 10.2* using the DEM generated from the 2006 aerial  
232 photographs. Following orthorectification, a pan-sharpened, natural colour multispectral  
233 image (3-band: Blue, Red Green) with a resolution of 0.5 m GSD per pixel was generated  
234 using the IHS method in *ArcMap* (Figure 3). The IHS method uses Intensity, Hue and  
235 Saturation Colour to merge the high-resolution panchromatic data (0.5 m GSD) with  
236 medium-resolution multispectral data (2.0 m GSD) in order to produce a multispectral image  
237 with higher-resolution properties.  
238  
239 For meaningful graphical and analytical purposes, the DEM data were converted into  
240 hillshaded relief models using *Spatial Analyst* in *ArcMap*. Hillshaded relief models were  
241 produced using an illumination angle of 30° and azimuths set at orthogonal positions of 45°  
242 and 315° (Figure 4). These properties have been extensively used in generating hillshaded  
243 relief models for the purposes of glacial geomorphological mapping and have been suggested  
244 as optimal settings for visualisation (e.g. Smith and Clark, 2005; Chen and Rose, 2008;  
245 Hughes et al., 2010; Boston, 2012; Pearce et al., 2014). Displaying the DEM data as  
246 hillshaded relief models with differing azimuths avoids azimuth bias and permits  
247 geomorphological features to be viewed under different lighting conditions, which can  
248 increase the visibility of subtle landforms (Smith and Clark, 2005; Pearce et al., 2014).



1  
2  
3  
4  
5  
6  
7  
8  
9  
10  
11  
12  
13  
14  
15  
16  
17  
18  
19  
20  
21  
22  
23  
24  
25  
26  
27  
28  
29  
30  
31  
32  
33  
34  
35  
36  
37  
38  
39  
40  
41  
42  
43  
44  
45  
46  
47  
48  
49  
50  
51  
52  
53  
54  
55  
56  
57  
58  
59  
60

249  
  
250  
  
  
  
  
251  
  
252  
  
253  
  
254  
  
255  
  
256  
  
257  
  
258  
  
259  
  
260  
  
261  
  
262  
  
263  
  
264  
  
265  
  
266  
  
267  
  
268  
  
269  
  
270  
  
271  
  
272

**3.2 Map production**

Detailed glacial geomorphological mapping was conducted from the imagery discussed above, combined with field investigations conducted in May and June 2014 to ground truth the desk-based mapping. This approach of applying multiple remote sensing datasets, augmented by field-based geomorphological investigations, has been extensively applied in the context of both glacierised and glaciated landscapes, encompassing a variety of geographical locations (e.g. Bennett et al., 2010; Boston, 2012; Bradwell et al., 2013; Reinardy et al., 2013; Brynjólfsson et al., 2014; Darvill et al., 2014; Evans et al., 2014, submitted; Jónsson et al., 2014; Pearce et al., 2014). The application of both the interpretation of remote sensing data and field surveys permits a holistic approach to mapping, wherein the advantages of each method can be combined to produce an accurate map with robust genetic interpretations (Brown et al., 2011; Boston, 2012).

Overlays of geomorphological features were digitally drawn in *ArcMap 10.2* using the remote sensing data, with individual vector layers created for each geomorphological feature. The initial interpretation of the remote sensing data and on-screen digitisation was then checked in the field. In order to enhance the accuracy of mapping and reduce errors which may arise from misinterpretation of features, examination of the remote sensing data was conducted both prior to and after the field investigations (cf. Lukas and Lukas, 2006; Boston, 2012; Pearce et al., 2014). The final digitised features were then exported to *Adobe Illustrator CC* for final editing and map production, along with a contour layer calculated at 20 m intervals using *Spatial Analyst* in *ArcMap* and the 2006 DEM to derive the elevation data. Following in the tradition of previous glacial geomorphological maps of Icelandic glacier

forelands, the glacier surface is represented on the maps by a mask generated directly from the processed imagery (cf. Evans, 2009).

## 4. Results

### 4.1 Moraine distribution and geomorphology

Glacial geomorphological mapping reveals a series of recessional (“annual”) moraines distributed across the Skálafellsjökull foreland, with a total of 3,201 moraine fragments mapped on the glacier foreland based on the 2012 satellite imagery. Long, largely uninterrupted sequences of moraines occur on the northern and central parts of the glacier foreland. Additionally, numerous “annual” moraines are evident in close proximity to the southeastern sector of the Skálafellsjökull margin. Comparison of the 2006 and 2012 maps of the glacier foreland reveals that moraine formation has occurred at both the southeastern and northeastern sectors of the Skálafellsjökull ice-margin, with 281 moraine fragments formed during this period. These individual moraine fragments form part of longer, discontinuous ridges that appear to reflect the geometry of the ice-margin. The mapping also indicates that this period of moraine formation coincides with a phase of substantial glacier retreat and ice-marginal lake expansion.

Following journal guidelines, detailed analysis of “annual” moraine properties are not presented here, but some characteristic features are briefly outlined. Further detailed analysis will be presented in a subsequent paper. The moraines typically take the form of discontinuous ridges, consisting of a number of smaller fragments which form part of longer chains (Figure 5). Crest-to-crest spacing (or longitudinal) spacing between individual chains of “annual” moraines ranges from ~5 m to 60 m on the Skálafellsjökull foreland. In planform, moraine ridges on the Skálafellsjökull foreland exhibit a distinctive “sawtooth” or crenulate

1  
2  
3 298 pattern, with teeth pointing in a down-ice direction and notches pointing upglacier (Figure 6;  
4  
5 299 cf. Matthews et al., 1979). Teeth exhibit maximum wavelengths and amplitudes of ~50 m and  
6  
7  
8 300 ~39 m, respectively, whilst notches exhibit maximum wavelengths and amplitudes of ~47 m  
9  
10 301 and ~41 m. Complexities in the general planview geometry occur locally, with individual  
11  
12 302 moraine ridges exhibiting bifurcations and cross-cutting patterns. The large-scale, sample  
13  
14 303 mapping of moraines in two selected areas (Maps 3 and 4) of the glacier foreland, based on  
15  
16 304 UAV-captured imagery, provides a clear visualisation of the characteristic planform  
17  
18 305 geometry and local complexities in this pattern. The “annual” moraines on the  
19  
20 306 Skálafellsjökull foreland are typically asymmetrical in cross-section, with cross-profiles  
21  
22 307 displaying shorter, steeper distal slopes and longer, gently-sloping ice-proximal surface  
23  
24 308 slopes. Individual moraines have heights ranging from ~0.2 m to 1.5 m, with moraine width  
25  
26 309 being between ~2 m and 18 m.  
27  
28  
29  
30  
31  
32

33  
34 311 ***4.2 Associated glacial geomorphological features***  
35  
36

37 312 Moraines on the Skálafellsjökull foreland are frequently found in close association with  
38  
39 313 flutings (Figure 7), which may extend on to the ice-proximal slopes of moraines in places.  
40  
41 314 Mapped flutings range in length from 7 m to 201 m, with a mean value of 42.8 m ( $n = 951$ ;  
42  
43 315 2012 imagery). On the reverse basalt bedrock slope near the southeastern sector of the  
44  
45 316 Skálafellsjökull margin, “annual” moraines and flutings are also found in association with an  
46  
47 317 abundance of roches moutonnées: flutings often extend from the lee-side faces of roches  
48  
49 318 moutonnées. This area of the glacier foreland is also characterised by a number of recessional  
50  
51 319 meltwater channels and a contemporary meltwater stream running along the ice-margin.  
52  
53 320 Locally, meltwater accumulates along parts of the southeastern margin to form a small ice-  
54  
55 321 marginal lake. At the time of the field surveys (May–June 2014), moraines in close proximity  
56  
57 322 to the contemporary ice-margin could be found partially submerged by ponded and slow-  
58  
59  
60

323 moving meltwater. The close association of flutings and “annual” moraines on the  
324 Skálafellsjökull foreland suggests the formation of these geomorphological features may be  
325 intimately linked, as has previously been suggested at Icelandic glaciers (cf. Boulton, 1976;  
326 Boulton and Hindmarsh, 1987; Benn, 1994; Evans and Twigg, 2002; Evans, 2003).

327

## 328 5. Summary and conclusions

329 Geomorphological mapping in this study, through a combination of desk- and field-based  
330 mapping, has resulted in the production of detailed, high-resolution glacial geomorphological  
331 maps showing the distribution of “annual” moraines and associated geomorphological  
332 features on the Skálafellsjökull foreland. The geomorphological mapping revealed a series of  
333 small-scale recessional (“annual”) moraines, with long sequences of moraines occurring on  
334 the northern and central parts of the glacier foreland. These “annual” moraines display  
335 distinctive “sawtooth” planform geometries (cf. Price, 1970; Matthews et al., 1979; Bradwell,  
336 2004). Complexities in the general pattern occur locally, with individual moraines exhibiting  
337 bifurcations and cross-cutting patterns. The inventory of geomorphological maps produced in  
338 this study provides a framework for subsequently exploring moraine chronology and  
339 sedimentology, from which recent ice-marginal fluctuations of Skálafellsjökull can be  
340 examined.

341

342 This study has also demonstrated potential of imagery captured using an Unmanned Aerial  
343 Vehicle (UAV) for the purposes of high-resolution mapping of small-scale geomorphological  
344 features. The acquisition of imagery using UAVs represents a potentially effective and low-  
345 cost technique for producing high-resolution, 3D georeferenced data (e.g. d’Oleire-Oltmanns  
346 et al., 2012; Hugenholtz et al., 2012, 2013; Lucieer et al., 2014) but its application in  
347 glaciology and glacial geomorphology has so far been limited (e.g. Whitehead et al., 2013;

1  
2  
3  
4  
5  
6  
7  
8  
9  
10  
11  
12  
13  
14  
15  
16  
17  
18  
19  
20  
21  
22  
23  
24  
25  
26  
27  
28  
29  
30  
31  
32  
33  
34  
35  
36  
37  
38  
39  
40  
41  
42  
43  
44  
45  
46  
47  
48  
49  
50  
51  
52  
53  
54  
55  
56  
57  
58  
59  
60

Ryan et al., 2015; Evans et al., submitted). In the context of contemporary glacial environments, UAV imagery represents a potentially valuable tool for repeat surveying and monitoring, allowing further insights into ice-frontal fluctuations and proglacial landscape evolution to be gained.

**Software**

Image processing was conducted in *Agisoft Photoscan Professional Edition*, whilst processing of GPS data was performed in *Leica Geo Office 8.3*. Desk-based geomorphological mapping was undertaken in *ESRI ArcMap 10.2*, with the mapping exported to *Adobe Illustrator CC* for final editing and map production.

**Acknowledgements**

This research was supported by a Quaternary Research Association (QRA) New Research Workers' Award, Van Mildert College (Durham University) Principal's Award and Van Mildert College Postgraduate Award. BMPC would like to thank Hannah Bickerdike, Jonathan Chandler and Bertie Miles for their assistance and companionship during fieldwork. Thanks are also due to Regína Hreinsdóttir (National Park Warden, South Territory) for granting permission to undertake fieldwork in the Vatnajökull National Park. Fieldwork was carried out under RANNÍS Agreement 4/2014.

**References**

Beedle, M. J., Menounos, B., Luckman, B. H., & Wheate, R. (2009). Annual push moraines as climate proxy. *Geophysical Research Letters*, 36, L20501. doi: <http://dx.doi.org/10.1029/2009GL039533>

- 372 Benn, D. I. (1994). Fluted moraine formation and till genesis below a temperate glacier:  
 373 Slettmarkbreen, Jotunheimen, Norway. *Sedimentology*, 41, 279–292. doi:  
 374 <http://dx.doi.org/10.1111/j.1365-3091.1994.tb01406.x>
- 375 Bennett, G. L., Evans, D. J. A., Carbonneau, P., & Twigg, D. R. (2010). Evolution of a  
 376 debris-charged glacier landsystem, Kvíárjökull, Iceland. *Journal of Maps*, 6(1), 40–  
 377 67. doi: <http://dx.doi.org/10.4113/jom.2010.1114>
- 378 Bennett, M. R. (2001). The morphology, structural evolution and significance of push  
 379 moraines. *Earth-Science Reviews*, 53, 197–236. doi: [http://dx.doi.org/10.1016/S0012-8252\(00\)00039-8](http://dx.doi.org/10.1016/S0012-8252(00)00039-8)
- 380
- 381 Björnsson, H., Pálsson, F., Guðmundsson, S., Magnússon, E., Adalgeirsdóttir, G.,  
 382 Jóhannesson, T., Berthier, E., Sigurðsson, O., & Thorsteinsson, T. (2013).  
 383 Contribution of Icelandic ice caps to sea level rise: Trends and variability since the  
 384 Little Ice Age. *Geophysical Research Letters*, 40, 1546–1550. doi:  
 385 <http://dx.doi.org/10.1002/grl.50278>
- 386 Boston, C. M. (2012). A glacial geomorphological map of the Monadhliath Mountains,  
 387 Central Scottish Highlands. *Journal of Maps*, 8(4), 437–444. doi:  
 388 <http://dx.doi.org/10.1080/17445647.2012.743865>
- 389 Boulton, G. S. (1976). The origin of glacially fluted surfaces: observations and theory.  
 390 *Journal of Glaciology*, 17, 287–309.
- 391 Boulton, G. S. (1986). Push moraines and glacier-contact fans in marine and terrestrial  
 392 environments. *Sedimentology*, 33, 677–698. doi: <http://dx.doi.org/10.1111/j.1365-3091.1986.tb01969.x>
- 393
- 394 Boulton, G. S., & Hindmarsh, R. C. A. (1987). Sediment deformation beneath glaciers:  
 395 rheology and sedimentological consequences. *Journal of Geophysical Research: Solid*  
 396 *Earth*, 92(B9), 9059–9082. doi: <http://dx.doi.org/10.1029/JB092iB09p09059>

- 397 Bradwell, T. (2004). Annual moraines and summer temperatures at Lambatungnajökull,  
 398 Iceland. *Arctic, Antarctic, and Alpine Research*, 36, 502–508. doi:  
 399 [http://dx.doi.org/10.1657/1523-0430\(2004\)036\[0502:AMASTA\]2.0.CO;2](http://dx.doi.org/10.1657/1523-0430(2004)036[0502:AMASTA]2.0.CO;2)
- 400 Bradwell, T., Sigurðsson, O., & Everest, J. (2013). Recent, very rapid retreat of a temperate  
 401 glacier in SE Iceland. *Boreas*, 42(4), 959–973. doi:  
 402 <http://dx.doi.org/10.1111/bor.12014>
- 403 Brown, V. H., Evans, D. J. A., & Evans, I. S. (2011). The Glacial Geomorphology and  
 404 Surficial Geology of the South-West English Lake District. *Journal of Maps*, 7(1),  
 405 221–243. doi: <http://dx.doi.org/10.4113/jom.2011.1187>
- 406 Brynjólfsson, S., Schomacker, A., & Ingólfsson, Ó. (2014). Geomorphology and the Little  
 407 Ice Age extent of the Drangajökull ice cap, NW Iceland, with focus on its three surge-  
 408 type outlets. *Geomorphology*, 213, 292–304. doi:  
 409 <http://dx.doi.org/10.1016/j.geomorph.2014.01.019>
- 410 Campbell, J. B., & Wynne, R. H. (2011). *Introduction to remote sensing* (Fifth Edition).  
 411 London: Taylor and Francis, 667 pp.
- 412 Chen, C., & Rose, J. (2008). Assessment of remote sensed imagery on the analysis of  
 413 landforms in Glen Roy. In Palmer, A. P., Lowe, J. J., & Rose, J. (Eds.), *The*  
 414 *Quaternary of Glen Roy and vicinity: Field guide* (pp. 36–45). London: Quaternary  
 415 Research Association.
- 416 Darvill, C. M., Stokes, C. R., Bentley, M. R., & Lovell, H. (2014). A glacial  
 417 geomorphological map of the southernmost ice lobes of Patagonia: the Bahía Inútil –  
 418 San Sebastián, Magellan, Otway, Skyring and Río Gallegos lobes. *Journal of Maps*,  
 419 10(3), 500–520. doi: <http://dx.doi.org/10.1080/17445647.2014.890134>



- 420 Davis, P. T., Briner, J. P., Coulthard, R. D., Finkel, R. W., & Miller, G. H. (2006).  
 421 Preservation of Arctic landscapes overridden by cold-based ice sheets. *Quaternary*  
 422 *Research*, 65(1), 156–163. doi: <http://dx.doi.org/10.1016/j.yqres.2005.08.019>
- 423 d'Oleire-Oltmanns, S., Marzolff, I., Peter, K. D., & Ries, J. B. (2012). Unmanned Aerial  
 424 Vehicle (UAV) for monitoring soil erosion in Morocco. *Remote Sensing*, 4(11), 3390–  
 425 3416. doi: <http://dx.doi.org/10.3390/rs4113390>
- 426 Dowdeswell, J. A., & Sharp, M. J. (1986). Characterization of pebble fabrics in modern  
 427 terrestrial glacial sediments. *Sedimentology*, 33, 699–710. doi:  
 428 <http://dx.doi.org/10.1111/j.1365-3091.1986.tb01970.x>
- 429 Evans, D. J. A. (2000). A gravel outwash/deformation till continuum, Skálafellsjökull,  
 430 Iceland. *Geografiska Annaler*, 82A(4), 499–512. doi: [http://dx.doi.org/10.1111/j.0435-](http://dx.doi.org/10.1111/j.0435-3676.2000.00137.x)  
 431 [3676.2000.00137.x](http://dx.doi.org/10.1111/j.0435-3676.2000.00137.x)
- 432 Evans, D. J. A. (2003). Ice-Marginal Terrestrial Landsystems: Active Temperate Glacier  
 433 Margins. In Evans, D. J. A. (Ed.), *Glacial Landsystems* (pp. 12–43). London: Arnold.
- 434 Evans, D. J. A. (2005). The glacier-marginal landsystems of Iceland. In Caseldine, C.,  
 435 Russell, A., Harðardóttir, J., Knudsen, Ó. (Eds.), *Iceland – Modern Processes and Past*  
 436 *Environments. Developments in Quaternary Sciences*, 5, 93–126.
- 437 Evans, D. J. A. (2009). Glacial Geomorphology at Glasgow. *Scottish Geographical Journal*,  
 438 125(3–4), 285–320. doi: <http://dx.doi.org/10.1080/14702540903364310>
- 439 Evans, D. J. A., Archer, S., & Wilson, D. J. H. (1999). A comparison of the lichenometric  
 440 and Schmidt hammer dating techniques based on data from the proglacial areas of  
 441 some Icelandic glaciers. *Quaternary Science Reviews*, 18(1), 13–41. doi:  
 442 [http://dx.doi.org/10.1016/S0277-3791\(98\)00098-5](http://dx.doi.org/10.1016/S0277-3791(98)00098-5)
- 443 Evans, D. J. A., Ewertowski, M., & Orton, C. Submitted. Fláajökull (north lobe), Iceland:  
 444 active temperate piedmont lobe glacial landsystem. *Journal of Maps*.



- 445 Evans, D. J. A., & Orton, C. (2015). Heinabergsjökull and Skalafellsjökull, Iceland: Active  
 446 Temperate Piedmont Lobe and Outwash Head Glacial Landsystem. *Journal of Maps*,  
 447 11(3), 415–431. doi: <http://dx.doi.org/10.1080/17445647.2014.919617>
- 448 Evans D. J. A., Phillips E. R., Hiemstra J. F. & Auton C. A. (2006). Subglacial till:  
 449 Formation, sedimentary characteristics and classification. *Earth-Science Reviews*,  
 450 78(1–2), 115–176. doi: <http://dx.doi.org/10.1016/j.earscirev.2006.04.001>
- 451 Evans, D. J. A., & Twigg, D. R. 2002. The active temperate glacial landsystem: a model  
 452 based on Breiðamerkurjökull and Fjallsjökull, Iceland. *Quaternary Science Reviews*,  
 453 21(20–22), 2143–2177. doi: [http://dx.doi.org/10.1016/S0277-3791\(02\)00019-7](http://dx.doi.org/10.1016/S0277-3791(02)00019-7)
- 454 Evans, D. J. A., Young, N. J. P., & Ó Cofaigh, C. (2014). Glacial geomorphology of  
 455 terrestrial-terminating fast flow lobes/ice stream margins in the southwest Laurentide  
 456 Ice Sheet. *Geomorphology*, 204, 86–113. doi:  
 457 <http://dx.doi.org/10.1016/j.geomorph.2013.07.031>
- 458 Forman, S. L., Mann, D. H., Miller, & G. H. (1987). Late Weichselian and Holocene relative  
 459 sea level history of Bröggerhalvoya, Spitsbergen. *Quaternary Research*, 27(1), 41–50.  
 460 doi: [http://dx.doi.org/10.1016/0033-5894\(87\)90048-2](http://dx.doi.org/10.1016/0033-5894(87)90048-2)
- 461 Gordon, J. E., & Sharp, M. (1983). Lichenometry in dating recent glacial landforms and  
 462 deposits, southeast Iceland. *Boreas*, 12(3), 191–200. doi:  
 463 <http://dx.doi.org/10.1111/j.1502-3885.1983.tb00312.x>
- 464 Hackney, C., & Clayton, A.I. (2015) Section 2.1.7: Unmanned Aerial Vehicles (UAVs) and  
 465 their application in geomorphic mapping. In Clarke, L. (Ed.) *Geomorphological*  
 466 *Techniques* (Online Edition). London: British Society for Geomorphology. ISSN:  
 467 2047-0371.
- 468 Hannesdóttir, H., Björnsson, H., Pálsson, F., Aðalgeirsdóttir, G., & Guðmundsson, S. (2014).  
 469 Variations of southeast Vatnajökull ice cap (Iceland) 1650–1900 and reconstruction of

- the glacier surface geometry at the Little Ice Age maximum. *Geografiska Annaler: Series A, Physical Geography*. doi: <http://dx.doi.org/10.1111/geoa.12064>
- Hättestrand, C., & Stroeven, A. P. (2002). A relict landscape in the centre of Fennoscandian glaciation: geomorphological evidence of minimal Quaternary glacial erosion. *Geomorphology*, 44, 127–143. doi: [http://dx.doi.org/10.1016/S0169-555X\(01\)00149-0](http://dx.doi.org/10.1016/S0169-555X(01)00149-0)
- Hugenholtz, C. H., Levin, N., Barchyn, T. E., & Baddock, M. C. (2012). Remote sensing and spatial analysis of aeolian sand dunes: a review and outlook. *Earth-Science Reviews*, 111(3–4), 319–334. doi: <http://dx.doi.org/10.1016/j.earscirev.2011.11.006>
- Hugenholtz, C. H., Whitehead, K., Brown, O. W., Barchyn, T. E., Moorman, B. J., LeClair, A., Riddell, K., & Hamilton, T. (2013). Geomorphological mapping with a small unmanned aircraft system (sUAS): feature detection and accuracy assessment of a photogrammetrically-derived digital terrain model. *Geomorphology*, 194, 16–24. doi: <http://dx.doi.org/10.1016/j.geomorph.2013.03.023>
- Hughes, A. L. C., Clark, C. D., & Jordan, C. J. (2010). Subglacial bedforms of the last British Ice Sheet. *Journal of Maps*, v2010, 543–563. doi: <http://dx.doi.org/10.4113/jom.2010.1111>
- Jónsson, S. A., Schomacker, A., Benediktsson, Í. Ö., Ingólfsson, Ó., & Johnson, M. D. (2014). The drumlin field and the geomorphology of the Múlajökull surge-type glacier, central Iceland. *Geomorphology*, 207, 213–220. doi: <http://dx.doi.org/10.1016/j.geomorph.2013.11.007>
- Krüger, J. (1995). Origin, chronology and climatological significance of annual moraine ridges at Mýrdalsjökull, Iceland. *The Holocene*, 5, 420–427. doi: <http://dx.doi.org/10.1177/095968369500500404>

- Landvik, J. Y., Ingólfsson, O., Mienert, J., Lehman, S. J., Solheim, A., Elverhøi, A., & Ottesen, D. (2005). Rethinking Late Weichselian ice sheet dynamics in coastal NW Svalbard. *Boreas*, 34, 7–24. doi: <http://dx.doi.org/10.1111/j.1502-3885.2005.tb01001.x>
- Lillesand, T. M., Kiefer, R. W., & Chipman, J. W. (2008). *Remote sensing and image interpretation* (Sixth Edition). Hoboken; John Wiley & Sons, 804 pp.
- Lucieer, A., Turner, D., King, D. H., & Robinson, S. A. (2014). Using an unmanned aerial vehicle (UAV) to capture micro-topography of Antarctic moss beds. *International Journal of Applied Earth Observation and Geoinformation*, 27(Part A), 53–62. doi: <http://dx.doi.org/10.1016/j.jag.2013.05.011>
- Lukas, S. (2012). Processes of annual moraine formation at a temperate alpine valley glacier: insights into glacier dynamics and climatic controls. *Boreas*, 41(3), 463–480. doi: <http://dx.doi.org/10.1111/j.1502-3885.2011.00241.x>
- Matthews, J. A., Cornish, R., & Shakesby, R. A. (1979). “Saw-tooth” moraines in front of Bødalsbreen, southern Norway. *Journal of Glaciology*, 88, 535–546.
- McKinzey, K. M., Orwin, J. F., & Bradwell, T. (2004). Re-dating the Moraines at Skálafellsjökull and Heinabergsjökull using different Lichenometric Methods: Implications for the Timing of the Icelandic Little Ice Age Maximum. *Geografiska Annaler*, 86A, 319–355. doi: <http://dx.doi.org/10.1111/j.0435-3676.2004.00235.x>
- Pearce, D., Rea, B. R., Bradwell, T., & McDougall, D. (2014). Glacial geomorphology of the Tweedsmuir Hills, Central Southern Uplands, Scotland. *Journal of Maps*, 10(3), 457–465. doi: <http://dx.doi.org/10.1080/17445647.2014.886492>
- Price, R. J. (1970). Moraines at Fjallsjökull, Iceland. *Arctic and Alpine Research*, 2(1), 27–42.

- Reinardy, B. T. I., Leighton, I., & Marx, P. J. (2013). Glacier thermal regime linked to processes of annual moraine formation at Midtdalsbreen, southern Norway. *Boreas*, 42(4), 896–911. doi: <http://dx.doi.org/0.1111/bor.12008>
- Rennen, M. (2004). Cocodati: Coordinate Conversion and Datum Transformation in Iceland Version 1.3. Online Software - Manual and Technical Reference. Iceland: Landmælingar Íslands, 28 pp. Available at: <http://cocodati.lmi.is/cocodati/cocodati-manual.pdf>.
- Ryan, J. C., Hubbard, A. L., Todd, J., Carr, J. R., Box, J. E., Christoffersen, P., Holt, T. O., & Snooke, N. (2015). Repeat UAV photogrammetry to assess calving front dynamics at a large outlet glacier draining the Greenland Ice Sheet. *The Cryosphere*, 9, 1–11. doi: <http://dx.doi.org/10.5194/tc-9-1-2015>
- Sharp, M. J. (1984). Annual moraine ridges at Skálafellsjökull, southeast Iceland. *Journal of Glaciology*, 30, 82–93.
- Sigurðsson, O. (1998). Glacier variations in Iceland 1930–1995: from the database of the Iceland Glaciological Society. *Jökull*, 45, 3–25.
- Sigurðsson, O., Jónsson, T., & Jóhannesson, T. (2007). Relation between glacier-termini variations and summer temperatures in Iceland since 1930. *Annals of Glaciology*, 42, 395–401. doi: <http://dx.doi.org/10.3189/172756407782871611>
- Smith, M. J., & Clark, C. D. (2005). Methods and visualization of digital elevation models for landform mapping. *Earth Surface Processes and Landforms*, 30, 885–900. doi: <http://dx.doi.org/10.1002/esp.1210>
- Snavely, N. (2008). *Scene reconstruction and visualization from Internet photo collections*. Unpublished PhD thesis, University of Washington, USA.
- Thórarinnsson, S. (1943). Oscillations of the Icelandic glaciers in the last 250 years. *Geografiska Annaler*, 25, 1–54.

1  
2  
3  
4  
5  
6  
7  
8  
9  
10  
11  
12  
13  
14  
15  
16  
17  
18  
19  
20  
21  
22  
23  
24  
25  
26  
27  
28  
29  
30  
31  
32  
33  
34  
35  
36  
37  
38  
39  
40  
41  
42  
43  
44  
45  
46  
47  
48  
49  
50  
51  
52  
53  
54  
55  
56  
57  
58  
59  
60

Verhoeven, G. (2011). Taking computer vision aloft – archaeological three-dimensional reconstructions from aerial photographs with Photoscan. *Archaeological Prospection*, 18, 67–73. doi: <http://dx.doi.org/10.1002/arp.399>

Westoby, M. J., Brasington, J., Glasser, N. F., Hambrey, M. J., & Reynolds, J.M. (2012). ‘Structure-from-Motion’ photogrammetry: A low-cost, effective tool for geoscience applications. *Geomorphology*, 179, 300–314. doi: <http://dx.doi.org/10.1016/j.geomorph.2012.08.021>

Whitehead, K., Moorman, B. J., & Hugenholtz, C. H. 2013. Brief Communication: Low-cost, on demand aerial photogrammetry for glaciological measurement. *The Cryosphere*, 7, 1879–1884. doi: <http://dx.doi.org/10.5194/tc-7-1879-2013>

## 568 List of Figures

569 Figure 1. (a) Field photograph of Skálafellsjökull descending from the Breiðabunga plateau  
 570 in eastern Vatnajökull (27.05.14). (b) Map showing the location of Skálafellsjökull, SE  
 571 Iceland. (c) Skálafellsjökull descends onto Hornafjörður coastal plain where it terminates as a  
 572 piedmont lobe. The contemporary ice-margin is fronted by a proglacial lake on  
 573 Heinabergsvötn.

574  
 575 Figure 2. Extracts from the principal remote sensing datasets employed for glacial  
 576 geomorphological mapping in this study. (a) Colour aerial photographs (0.41 m GSD) from  
 577 2006, *Loftmyndir ehf.* (b) Panchromatic satellite image (0.5 m GSD) from the WorldView-2  
 578 sensor, *European Space Imaging* (June 2012). (c) Multispectral satellite image (2.0 m GSD)  
 579 from the WorldView-2 sensor, *European Space Imaging* (June 2012). (d) DEM data  
 580 visualised as a hillshaded relief model, generated from UAV-captured imagery.

581  
 582 Figure 3. Comparison of the processed satellite imagery used in this research. (a)  
 583 Panchromatic satellite image (0.5 m GSD). (b) Multispectral satellite image (2.0 m GSD). (c)  
 584 Pansharpened 3-band natural colour image (0.5 m GSD).

585  
 586 Figure 4. Extracts from hillshaded relief models showing “annual” moraines on the foreland  
 587 of Skálafellsjökull. The models are derived from the UAV-captured imagery. (a) Hillshaded  
 588 relief model generated using an illumination angle of 30° and an azimuth of 45°. (b)  
 589 Hillshaded relief model generated using an illumination angle of 30° and an azimuth of 315°.  
 590 The difference in appearance of the “annual” moraines between the two models is apparent,  
 591 demonstrating the value of visualising the data with different azimuths.

592

1  
2  
3  
4  
5  
6  
7  
8  
9  
10  
11  
12  
13  
14  
15  
16  
17  
18  
19  
20  
21  
22  
23  
24  
25  
26  
27  
28  
29  
30  
31  
32  
33  
34  
35  
36  
37  
38  
39  
40  
41  
42  
43  
44  
45  
46  
47  
48  
49  
50  
51  
52  
53  
54  
55  
56  
57  
58  
59  
60

Figure 5. Histogram and summary statistics of mapped moraine lengths for the entire dataset. Box-and-whisker plots show the 25th and 75th percentiles (grey box), and the 5th and 95th percentiles (whisker ends). The mean (horizontal line) is also shown.

Figure 6. Field photograph showing the characteristic “sawtooth” planform of moraines on the Skálafellsjökull foreland.

Figure 7. Field photograph across the southern part of the Skálafellsjökull foreland showing the close association of moraines and flutings.



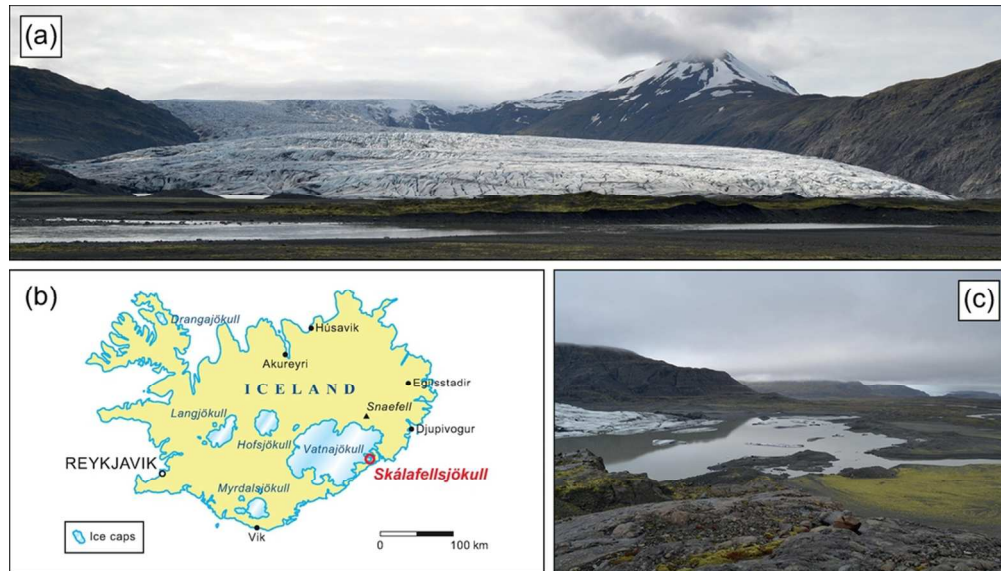


Figure 1. (a) Field photograph of Skálafellsjökull descending from the Breiðabunga plateau in eastern Vatnajökull (27.05.14). (b) Map showing the location of Skálafellsjökull, SE Iceland. (c) Skálafellsjökull descends onto Hornafjörður coastal plain where it terminates as a piedmont lobe. The contemporary ice-margin is fronted by a proglacial lake on Heinabergsvötn.

88x50mm (300 x 300 DPI)



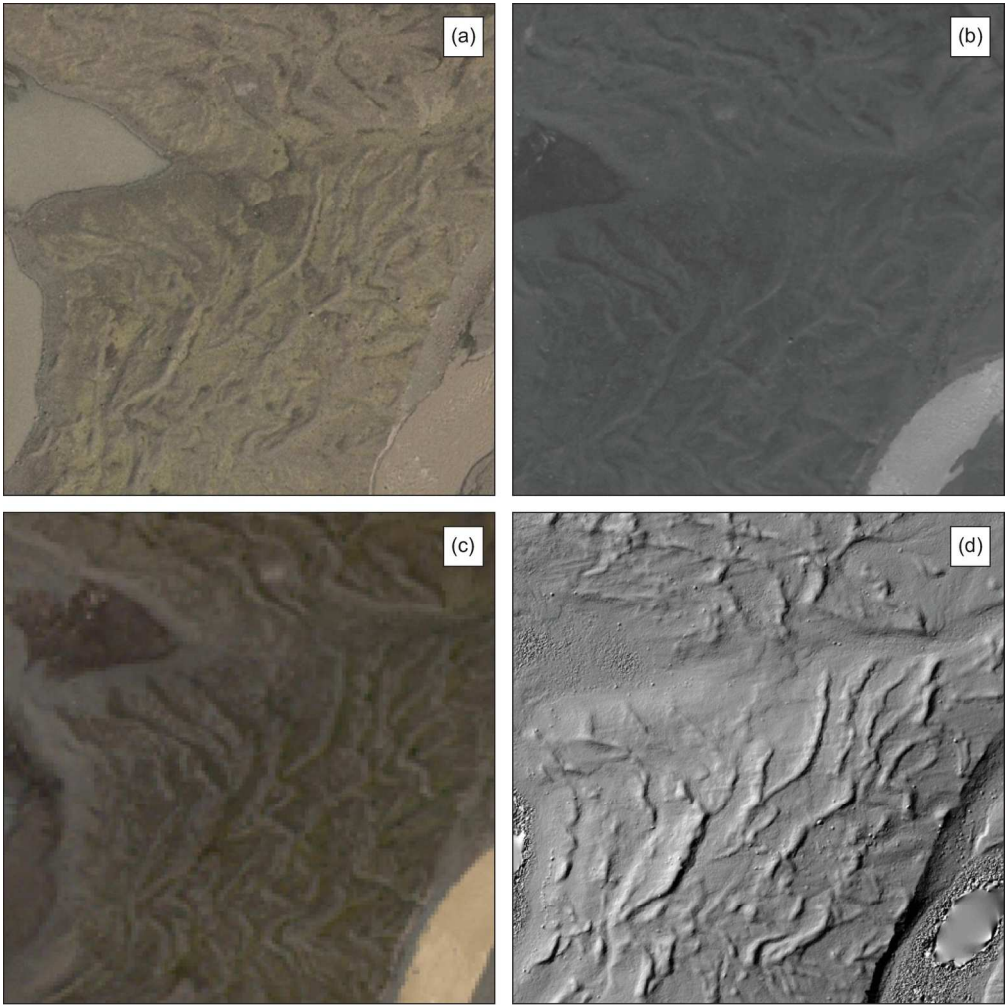


Figure 2. Extracts from the principal remote sensing datasets employed for glacial geomorphological mapping in this study. (a) Colour aerial photographs (0.41 m GSD) from 2006, Loftmyndir ehf. (b) Panchromatic satellite image (0.5 m GSD) from the WorldView-2 sensor, European Space Imaging (June 2012). (c) Multispectral satellite image (2.0 m GSD) from the WorldView-2 sensor, European Space Imaging (June 2012). (d) DEM data visualised as a hillshaded relief model, generated from UAV-captured imagery. 174x174mm (300 x 300 DPI)

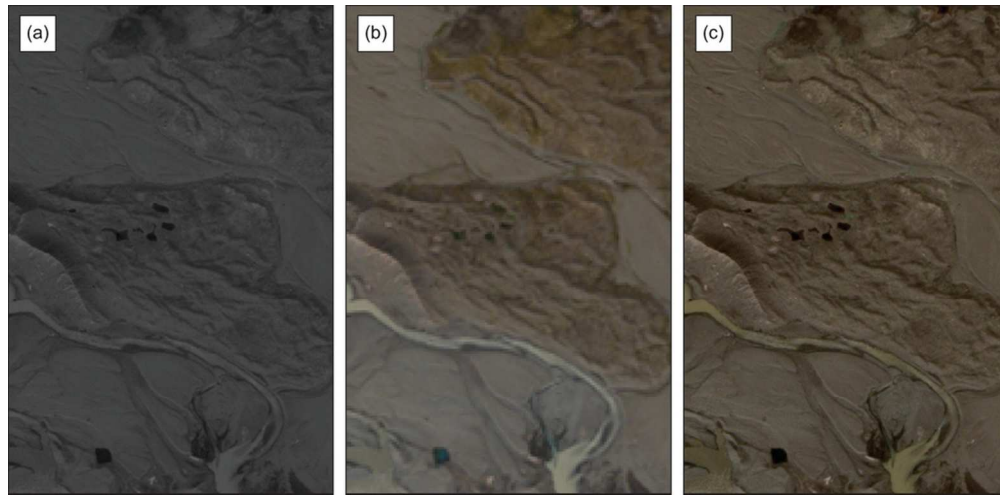


Figure 3. Comparison of the processed satellite imagery used in this research. (a) Panchromatic satellite image (0.5 m GSD). (b) Multispectral satellite image (2.0 m GSD). (c) Pansharpened 3-band natural colour image (0.5 m GSD).  
93x45mm (300 x 300 DPI)

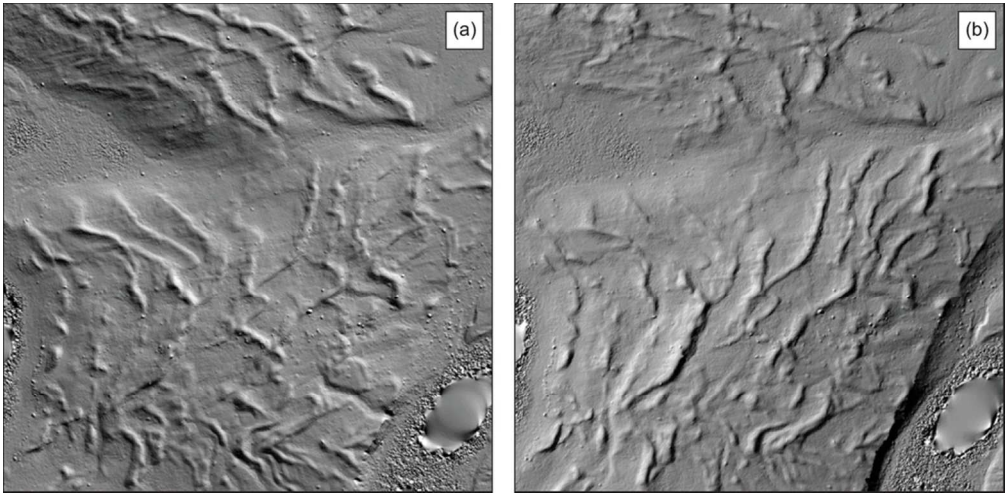


Figure 4. Extracts from hillshaded relief models showing “annual” moraines on the foreland of Skálafellsjökull. The models are derived from the UAV-captured imagery. (a) Hillshaded relief model generated using an illumination angle of 30° and an azimuth of 45°. (b) Hillshaded relief model generated using an illumination angle of 30° and an azimuth of 315°. The difference in appearance of the “annual” moraines between the two models is apparent, demonstrating the value of visualising the data with different azimuths.

90x44mm (300 x 300 DPI)

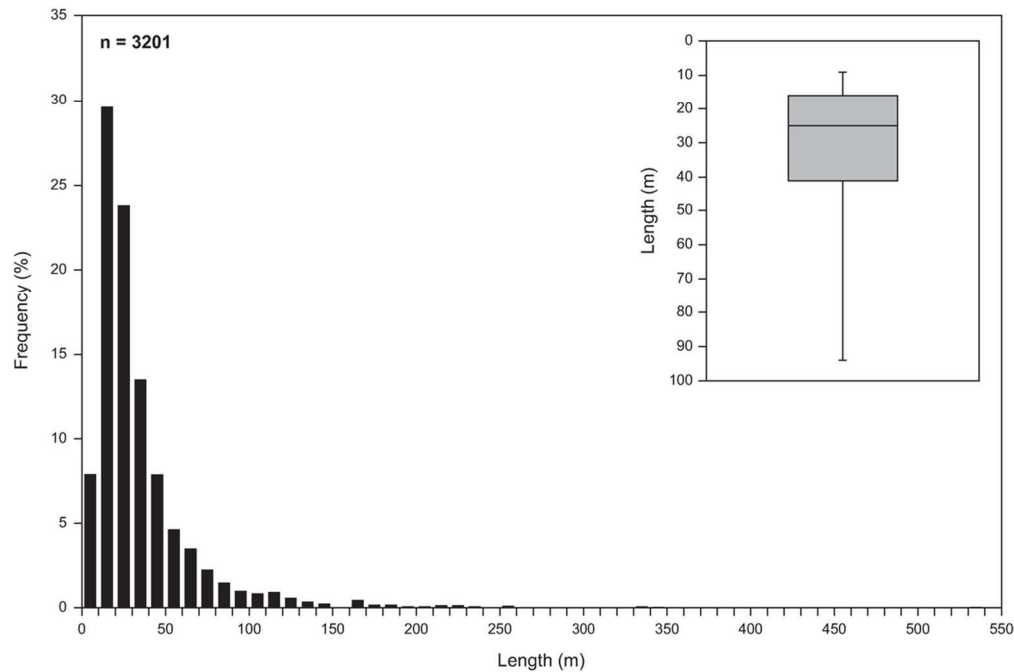


Figure 5. Histogram and summary statistics of mapped moraine lengths for the entire dataset. Box-and-whisker plots show the 25th and 75th percentiles (grey box), and the 5th and 95th percentiles (whisker ends). The mean (horizontal line) is also shown.

103x69mm (300 x 300 DPI)

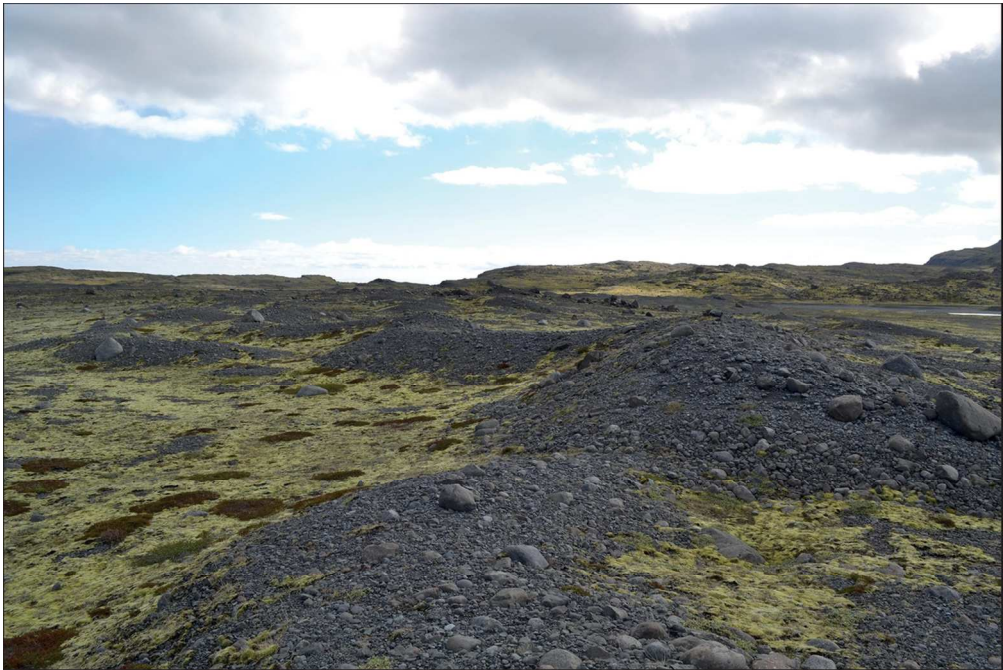


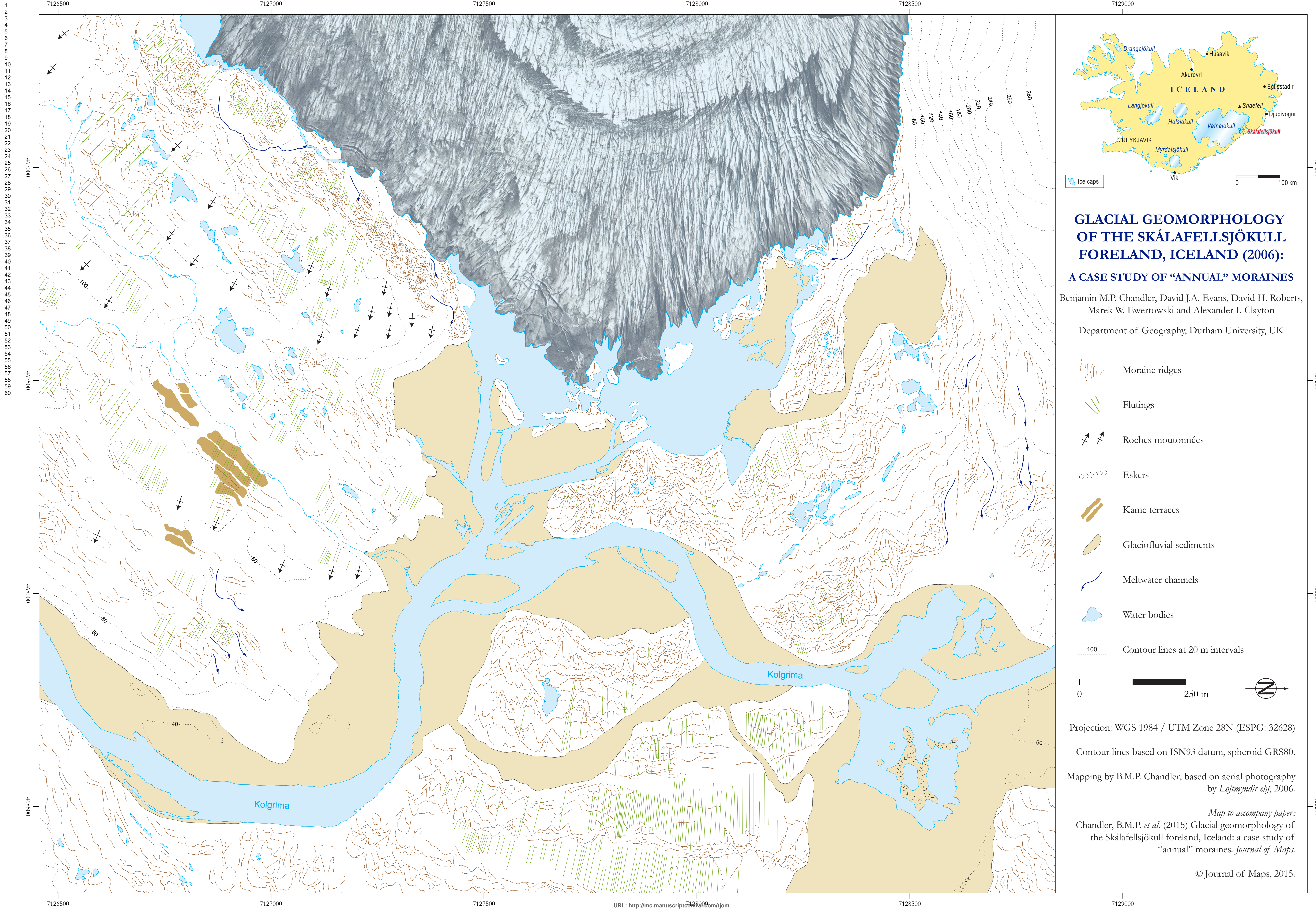
Figure 6. Field photograph showing the characteristic “sawtooth” planform of moraines on the Skálafellsjökull foreland.  
114x76mm (300 x 300 DPI)





Figure 7. Field photograph across the southern part of the Skálafellsjökull foreland showing the close association of moraines and flutings.  
115x77mm (300 x 300 DPI)





# GLACIAL GEOMORPHOLOGY OF THE SKÁLAFELLSJÖKULL FORELAND, ICELAND (2006): A CASE STUDY OF “ANNUAL” MORAINES

Benjamin M.P. Chandler, David J.A. Evans, David H. Roberts, Marek W. Ewertowski and Alexander I. Clayton

Department of Geography, Durham University, UK

- Moraine ridges
- Flutings
- Roches moutonnées
- Eskers
- Kame terraces
- Glaciofluvial sediments
- Meltwater channels
- Water bodies
- Contour lines at 20 m intervals

0 250 m

Projection: WGS 1984 / UTM Zone 28N (ESPG: 32628)

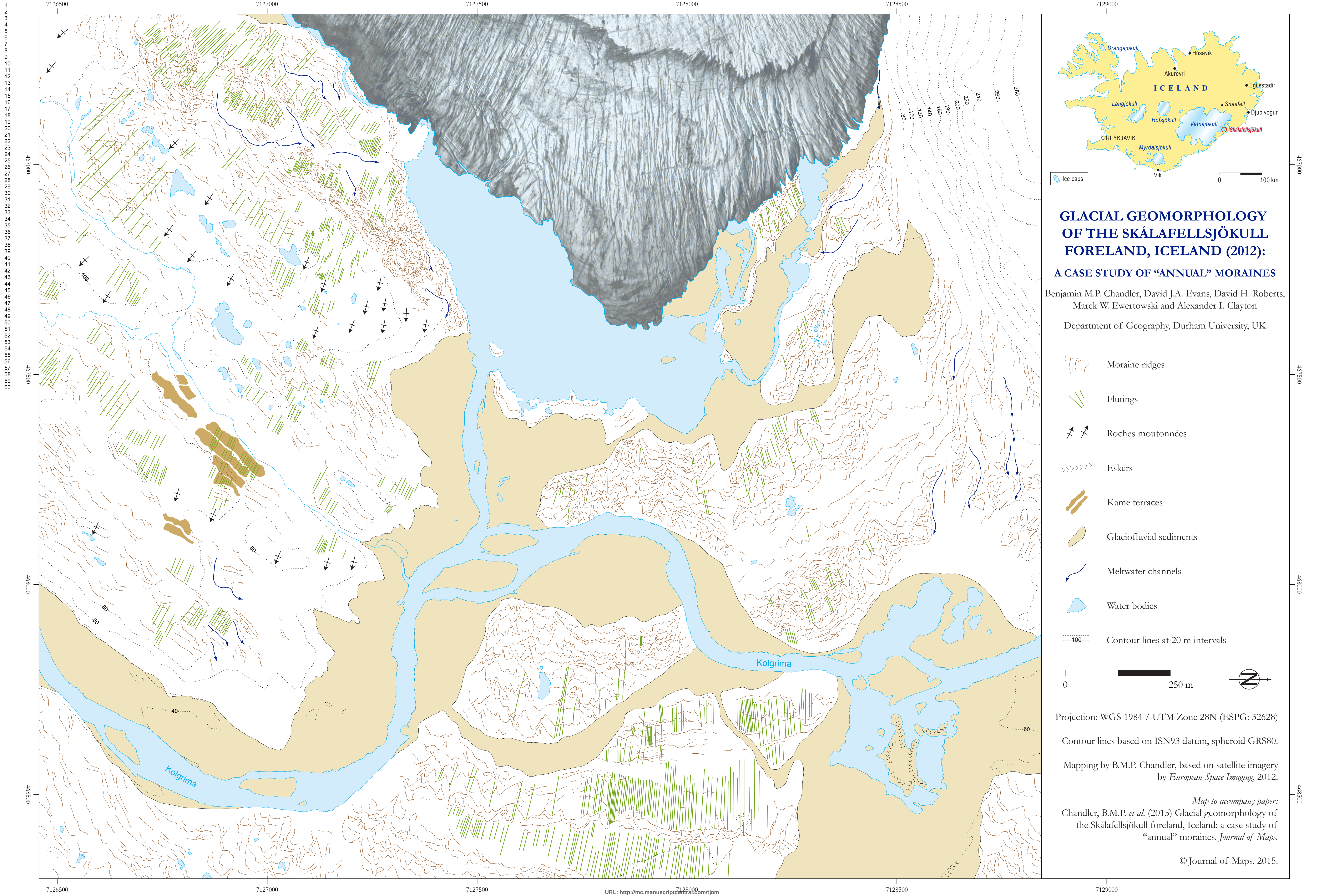
Contour lines based on ISN93 datum, spheroid GRS80.

Mapping by B.M.P. Chandler, based on aerial photography by *Loftmyndir ehf*, 2006.

Map to accompany paper:  
Chandler, B.M.P. *et al.* (2015) Glacial geomorphology of the Skálafellsjökull foreland, Iceland: a case study of “annual” moraines. *Journal of Maps*.

© Journal of Maps, 2015.







GLACIAL GEOMORPHOLOGY OF THE SKÁLAFELLSJÖKULL FORELAND, ICELAND (2013):  
A CASE STUDY OF “ANNUAL” MORAINES

Benjamin M.P. Chandler, David J.A. Evans, David H. Roberts, Marek W. Ewertowski and Alexander I. Clayton  
Department of Geography, Durham University, UK

© Journal of Maps, 2015.





Benjamin M.P. Chandler, David J.A. Evans, David H. Roberts, Marek W. Ewertowski and Alexander I. Clayton  
Department of Geography, Durham University, UK

© Journal of Maps, 2015.

